Fuel 220 (2018) 503–512

Contents lists available at ScienceDirect

Fuel

journal homepage: www.elsevier.com/locate/fuel

Full Length Article

Investigating molecular conformation and packing of oxidized asphaltene molecules in presence of paraffin wax

Alireza Samieadel[a], Daniel Oldham[b], Elham H. Fini[c,*]

[a] Department of Energy and Environmental Systems, North Carolina A&T State University, 1601 E Market St, Greensboro, NC 27411, United States
[b] Joint School of Nanoscience and Nanoengineering, North Carolina A&T State University, 2907 East Gate City Blvd, Greensboro, NC 27401, United States
[c] Department of Civil, Architectural, and Environmental Engineering, North Carolina A&T State University, 1601 McNair Hall, Greensboro, NC 27405, United States

ARTICLE INFO

Keywords:
Oxidized asphalt binder
Paraffin wax
Molecular packing
Diffusion
Molecular dynamics simulation
Aggregation

ABSTRACT

This study investigates the effect of paraffinic wax (as a base component in many commercial rejuvenators) on the rheological and intermolecular properties of aged asphalt binder. Samples of oxidized asphalt binder doped with (1%, 3%, 5%, and 10%) paraffin wax were characterized using the rotational viscometer (RV), dynamic shear rheometer (DSR), bending beam rheometer (BBR) and direct tension test (DTT). The RV results showed an improvement trend in workability of aged binder as wax content increased. The DSR results (for a temperature range of 10–76 °C) showed lower complex modules for wax-doped specimen than control specimen. The BBR test results performed at sub-zero temperature showed that an increase of wax dosage led to higher creep stiffness modulus indicating that the asphalt binder became generally stiffer in presence of wax at low temperature. However, fracture energy measured through DTT test showed a significant reduction in presence of wax. The latter can be attributed to plausible weak secondary bonds between wax and asphaltene molecules as well as crystallization of wax molecules at low temperature within the asphalt matrix. This in turn can lead to wax crystals playing as stress localization point giving rise to crack nucleation at the wax-asphalt interface reducing overall fracture energy; it was further observed that as the wax content increased, the asphalt binder became more brittle.

To further investigate the effect of wax on the molecular conformation and packing in aged asphalt binder, a molecular simulation was performed on a system of wax and oxidized asphaltene. The results of molecular simulations showed a reduction in formation of oxidized asphaltene nano-aggregates as the amount of wax increased in the wax-doped oxidized asphaltene matrix at room temperature, which was also confirmed by size exclusion chromatography. Furthermore, the radial distribution function results showed a less packed structure of oxidized asphaltene molecules in presence of wax molecules. Increasing the wax content also increased the diffusion coefficient of wax into the oxidized asphaltene matrix within a solvent medium. It was also showed that interaction energy of a dimer of oxidized asphaltene is at a lower energy state in presence of wax molecules, which suggests that wax molecules can promote dimerization of oxidized asphaltene molecules while suppressing nano-aggregates formation.

1. Introduction

Known as a good adhesive in the construction sector, asphalt binder has been used in more than 90 percent of paved roads in the U.S. [27,46]. The asphalt binder used in hot mix asphalt is always susceptible to reaction with oxygen in the air, a process called oxidative aging [34,52].

Oxidative aging is a major factor responsible for hardening and rheological changes in asphalt, resulting in degradation of desirable asphalt properties [8,13,44,47]. The oxidative aging process happens in two stages; for each stage, there is a laboratory test method to simulate it. The rolling thin-film oven (RTFO) test is used to simulate short-term aging that happens during the construction phase; the pressured aging vessel (PAV) test is used to simulate long-term aging of asphalt binder [11,19,36,40,49]. The use of reclaimed asphalt pavement (RAP) has been highly promoted by both road authorities and asphalt contractors; mainly due to increase and fluctuation of asphalt binder price from $235 per ton in 2006 to $635 in 2015 and to $409 in 2018 based on asphalt price index [28]. Another motivation for promoting use of RAP is its abundance in the US., as well as the potential environmental

* Corresponding author.
E-mail addresses: asamiead@aggies.ncat.edu (A. Samieadel), djoldham@aggies.ncat.edu (D. Oldham), efini@ncat.edu (E.H. Fini).

https://doi.org/10.1016/j.fuel.2018.02.031
Received 21 September 2017; Received in revised form 4 February 2018; Accepted 6 February 2018

benefit from reduction of use of natural resources and virgin bitumen which can off-set some of the consumption of depleting resources of virgin binder and mineral aggregate [30].

To allow usage of high RAP asphalt mixture, a rejuvenator is needed to retrieve the original mechanical properties of virgin asphalt binder. Currently, different types of rejuvenator for aged asphalt have been introduced to the market; these rejuvenators have different origins such as bio-based (wood pellets, animal waste, soybean and corn stover), waste engine oil, and some refinery-based oils that have portions of paraffinic oil bases [53,9,29]. N-alkane is a saturated hydrocarbon (C_nH_{2n+2}) (also called wax) that can be in form of a gas for n less than 5, a liquid for n between 5 and 17, and a solid for n greater than 17 [16]. Many newly used rejuvenators contain paraffinic wax or paraffinic oil [25]; these still have the viscosity-lowering effect, but there is still the question of their effectiveness in chemically rejuvenating aged asphalt. Previous researches studied rejuvenators which contained paraffinic oil base. Mogawer et al. [25] used paraffinic oil as rejuvenator and showed that it improved cracking properties of asphalt mixtures containing 50% RAP binder. For instance fatigue test shows a much higher number of cycles (two times of control binder) to failure point. Zaumanis et al. [53] introduced waste engine oil with paraffin wax to mixtures made from 100% RAP binder; the latter showed improvement in creep compliance which was increased by 25% compared to reference binder. Wang et al. [50] used a warm mix additive with structure of a polyethylene wax as rejuvenator for high RAP mixtures and showed improvement of high and low temperature properties.

Among the four different chemical groups known as SARA (saturates, aromatics, resins and asphaltenes) [14], asphaltenes are the highly polar constituents of asphalt binder that are dispersed in the maltene phase [1]. A change in the concentration of asphaltenes in asphalt binder causes a variety of changes in the asphalt's rheology as well as the asphalt's mechanical properties [18]. The asphaltene molecules and their self-interaction are recognized to strongly affect the rheological and mechanical behavior of asphalt binder [22,26]. During the aging process of asphalt binder, one of the major factors that contributes to the stiffening of asphalt binder is the oxidation of polar aromatics, and asphatenes, leading to an increased aggregation due in polar fraction of asphalt components [42]. It has been documented that oxidation increases the asphaltene fraction of binder as the aromatics convert to asphaltenes [35]. The results of gel permeation chromatography (GPC) indicated an increase in high molecular size species after asphalt was exposed to oxidation; the latter was attributed to asphaltene molecules becoming more prone to aggregation due to oxidation [39].

Other studies focused on examining interactions of wax with other constituents of asphalt binder in micro scale [12,15,33,38]. The effects of paraffin wax on unaged asphalt binder at both macro scale and nano scale was also studied by [37]. However, the effect of paraffin wax materials on aged asphalt binder and understanding the connection between molecular interactions and rheological properties of aged asphalt is yet to be investigated.

Furthermore, there are limited study of the effect of wax on asphaltene behavior (as one of the key players of asphalt properties), especially after oxidation of asphaltene during aging process, and its effect on asphaltene nano-aggregates formation.

This paper examines molecular conformation and packing of oxidized asphaltene molecules in presence of paraffin wax via both computational modeling and experiments. Accordingly, the paper presents a comprehensive thermos-mechanical characterization aged asphalt binder doped with different dosages of paraffin wax utilizing a rotational viscometer, a dynamic shear rheometer, a bending beam rheometer, and a direct tension test. The Size exclusion chromatography was done to study the effect of paraffin wax on the formation of nanoparticles. To further study the intermolecular interactions between paraffin wax and aged asphaltene molecules, an equilibrium molecular dynamics simulation has been performed using Large-scale Atomic and Molecular Parallel software in the MedeA® 2.2 environment. The simulations took place on a simplified model of the wax and oxidized asphaltene complex in two stage: first, the effect of doped n-Paraffin wax on the self-association of oxidized asphaltene molecules was studies; second the behavior of wax molecules in a complex of asphaltene-wax in methanol as a solvent medium was studied. The result of this study provides in-depth understanding on how paraffin wax affects molecular packing of oxidized asphalt binder, and consequently its thermo-mechanical properties.

2. Experiment details

2.1. Experiment plan

The asphalt binder used in this study was graded as PG 64–22 and donated by Associated Asphalt Inc. of Greensboro NC; it was aged based on RTFO (short term aging simulator) and PAV (long term aging simulator) based on the standards [2,5] and doped with different paraffin wax dosages. For the aging process, the binder was initially aged using a rolling thin-film oven followed by two durations of the regular aging procedure of a pressure aging vessel. The test using two durations is known as 2XPAV, total of 40 h. 2XPAV has been shown to give better results with regard to the long-term aging that happens in the field [8]. The wax that was used for aged asphalt binder modification was a petroleum based paraffin wax (P31, with melting point of 53–57 °C, purchased from Fischer Scientific). The wax was blended at 1%, 3%, 5%, and 10 %wt of the initial aged asphalt binder, and samples were hand-blended at 135 °C for 30 min.

The viscosity results were determined using a rotational viscometer (RV). Measurements were conducted following ASTM D4402 [3] using a Brookfield Viscometer RV-DVIII Ultra, by applying a rotational shear on the selected material. Samples were prepared by pouring 10.5 g of each sample (aged binder with different concentrations) into an aluminum chamber following by cooling to room temperature. Samples were preheated in an oven for 30 min before testing in the temperature-controlled thermoset apparatus. After reaching thermal equilibrium, three viscosity results were taken at three-minute intervals until the results had a range of less than 100 cP (0.1 Pa·s). The average value of three readings was taken as the viscosity value. The speed chosen for this study was 20 rpm performed at 120, 135, and 150 °C.

The complex moduli results were determined using the Malvern Kinexus Pro dynamic shear rheometer (DSR) following ASTM D7552 – 09 [7]. Each sample (three replicates for each sample was tested) was test at 31 different frequencies ranging from 0.1 to 100 rad/s at a temperature range of 76–10 °C with 6-degree increments. The 25 mm spindle was used for the high intermediate temperature range of 64–76 °C, while the 8 mm spindle was used for 58–10 °C due to increased stiffness of the binder at lower temperatures [20]. From the resulting data, master curves were generated using the principle of time–temperature superposition (TTS) using the Williams-Landel-Ferry method (WLF) [51] at a reference temperature of 43 °C. Furthermore, the temperature at which the loss moduli and storage moduli meet (known as the crossover temperature) was measured as a property of the material. In general, viscoelastic materials with higher crossover temperature reach their elastic behavior faster as temperature drops and behave more as a stiffer material [17,37].

The bending beam rheometer (BBR) was used to evaluate the modified aged binder's stiffness and ability to relax (m-value) at low temperature and compare it to that of unmodified aged binder. For the low-temperature testing, −12 °C was selected, following the SuperPave binder PG specification, which requires the binder to be tested at the low-temperature grade of the binder (PG 64-22) plus 10 °C, as mentioned in ASTM D6648 [6]. Asphalt binder sample beams were prepared by pouring the binder into aluminum molds (four replicates). The samples were allowed one hour to cool to room temperature, then placed in a freezer for five minutes before being demolded. A constant

load of 100 g was applied on the middle point of specimens as the deflection was measured continuously.

The direct tension test (DTT) was used to study low-temperature stress and strain and fracture properties of the modified aged binder. Six dog-bone-shaped binder specimens were prepared (dimensions of 40 mm long, 6 mm width, and 6 mm thick) according to ASTM D6723 [4]. The binder was poured into aluminum molds (six replicates for each sample), allowed to cool to room temperature for one hour, and then trimmed and placed in a freezer for seven minutes before demolding, to prevent deflection. The samples were then placed in the DTT's cooling bath at -12 °C, following SuperPave binder PG specification (ASTM D6723-12) [4]. Samples remained at −12 °C for one hour for thermal equilibrium. The test started when the load reached 2 N with a strain rate of 3 percent/min. During the test, load and displacement of the sample up to failure point were recorded and then used to calculate fracture energy (the amount of energy required to create two new surfaces) and ductility (the change in length divided by the original length).

The Size Exclusion Chromatography (SEC) analysis was conducted using a Thermofisher RefractoMax 521 RI detector and Malvern H100-3078 column (7.8 mm × 300 mm). A WPS-3000TSL analytical autosampler was fully controlled by the Chromeleon chromatography management system. Samples (3% w/w in Tetrahydrofuran, THF) were filtered using 0.45-μm Millipore PTFE to remove suspended particulates; a pump flow rate of 1.0 mL/min with THF as the carrier solvent and injection volumes of 25 μL were used. The separation of the multi-component mixture took place in the column. A constant flow of fresh eluent was supplied to the column via a pump to detect analytes. The analysis was conducted based on size separation of analytes. The resulting chromatographic data was processed using Chromeleon software.

3. Results and data analysis

3.1. Experiment results

3.1.1. Viscosity

The effect of wax content on the viscosity aged asphalt binder was investigated at different temperatures (Fig. 1). The viscosity results show that by increasing the wax concentration from 1% to 10%, the viscosity of the blend decreases. Furthermore, the increase in temperature shows a swift reduction in binder viscosity. The viscosity difference for different dosages also decreases as the temperature increases. This change in viscosity at high temperatures occurs when wax crystals can't be formed and the wax molecules can move freely in the binder medium.

3.1.2. Complex modulus and crossover temperature

Using the dynamic shear rheometer (DSR), the complex modulus (G^*) master curves for 0%, 1%, 3%, 5%, and 10% wax-modified aged binder were calculated and plotted in Fig. 2-a. The results indicate that at a higher percentage of wax content, the aged asphalt binder becomes softer, especially for 5% and 10% wax. This softening effect is more noticeable at lower temperatures. At lower temperatures (higher frequencies), the binder becomes softer with an increase of wax content, while at higher temperatures, there is not much change after 5% wax. The results show that, for a temperature range of 10–76 °C, adding more than 3% wax is needed before a noticeable softening effect in aged asphalt binder starts.

To investigate the aforementioned phenomenon more closely using the DSR, the point at which the storage and loss moduli intersect (at a phase angle of 45°) was also determined as an indicator of the hardness of a material. This point is also known as the crossover temperature and is a physical property of a material. The crossover temperatures of unmodified aged binder, and aged with different wax concentrations are presented in Fig. 2-b. The crossover temperatures show that by aging the asphalt binder, the crossover temperature of the material increases significantly. By adding wax to aged material, a small reduction is observerd at lower concentrations followed by an increase at higher dosages. This can be related to the formation of wax crystals at lower temperatures than its melting point.

3.1.3. Stiffness and M-value

Fig. 3 shows the stiffness and m-value results that were determined using the BBR. The stiffness results (left axis) show that an increase in wax content leads to a higher stiffness value in which by adding 10% wax the stiffness increases by almost 30%. This phenomenon can be due to an increase in the formed crystallized networks of the paraffin wax in the bulk of aged asphalt binder. This is also shown with the modified aged binder's decreased ability to relax stress, as shown by the constant decreasing of the m-value up to 20% less than unmodified aged binder after adding 10% paraffin wax (right axis).

3.1.4. Fracture energy and ductility

Fig. 4-a shows the fracture energy obtained from a DTT test by calculating the area under the curve of load–displacement. The fracture energy represents the cohesive strength of the material and the energy that is needed to bring the material to cohesive failure. The results indicate that by adding wax to aged asphalt binder, the material becomes extremely brittle. The results from ductility also show that by adding wax, the ductility of aged material decreases by 30 percent (Fig. 4-b). A lower peak load along with lower fracture energy and

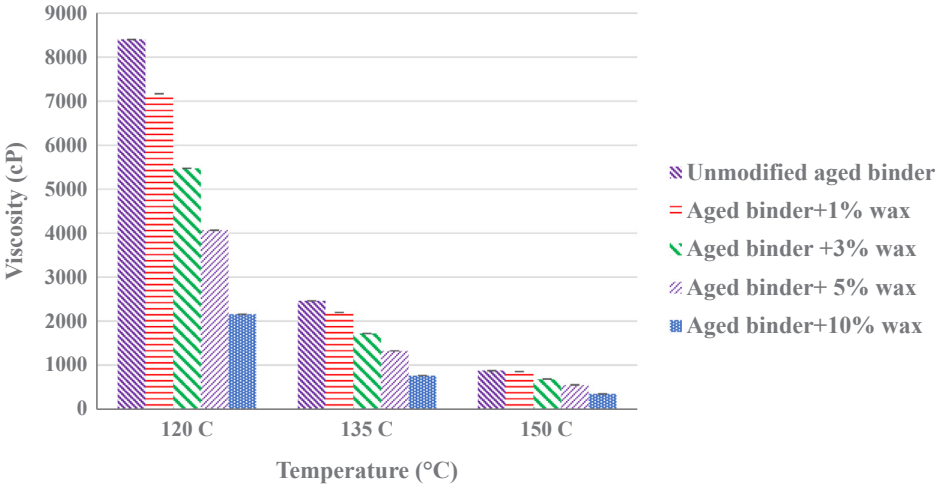

Fig. 1. Viscosity vs temperature at 0%, 1%, 3%, 5% and 10% wax under 20 rpm.

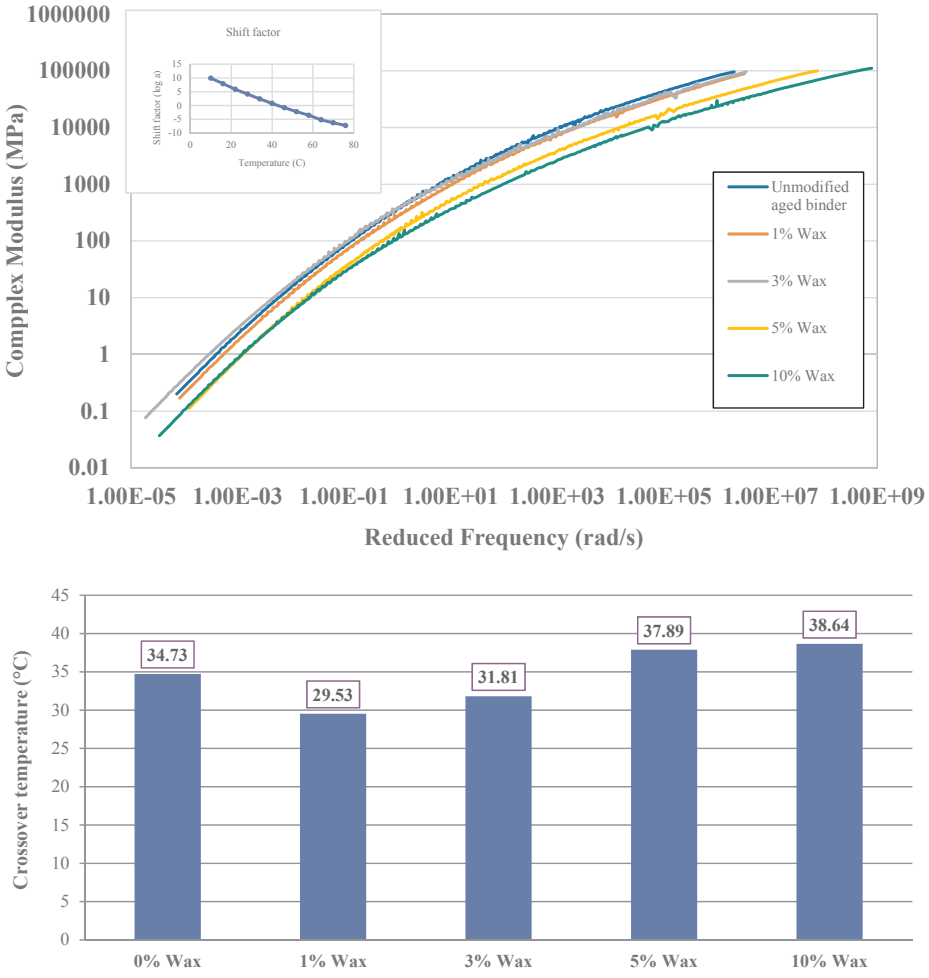

Fig. 2. Results for 0%, 1% 3%, 5% and 10% wax-modified aged binder: (a-top) complex modulus, (b – bottom) crossover temperature.

ductility does not show any improvement from added wax in aged asphalt binder's low-temperature rheological properties.

This change in properties of aged binder can be explained as being caused by the formation of more weak crystal networks inside the bulk of aged asphalt binder which decrease the resistance of binder from tensile stress. The reason for ununiform trend for fracture test is the fact that mechanism for destructive tests are different from the non-destructive tests as DSR showing a more consistent trend with increase of wax content. This further confirms that at specific wax content fracture mechanism transitions from bulk fracture to a crack growth at the interface between wax and asphalt

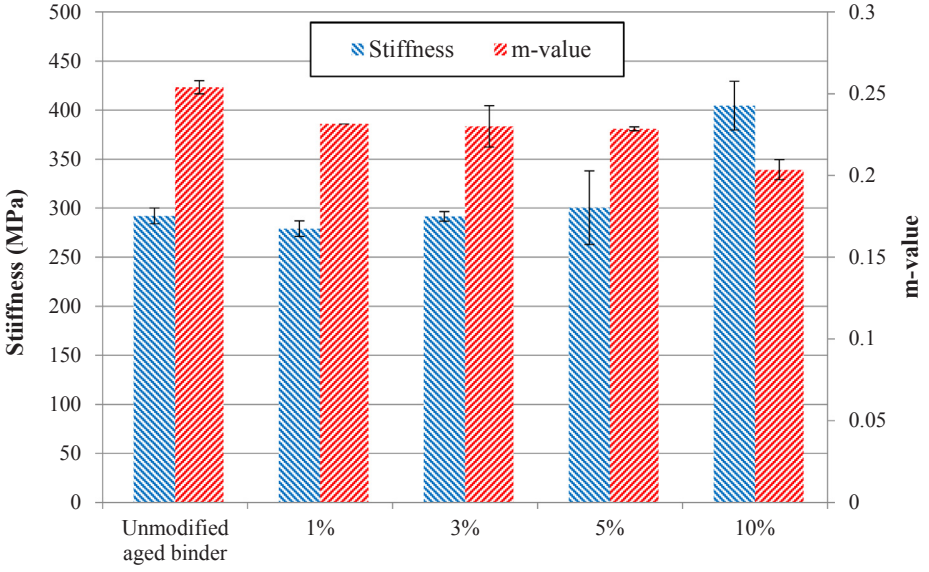

Fig. 3. Stiffness and m-value results for unmodified aged binder, 0%, 1%, 3%, 5%, and 10% wax-modified aged asphalt binder.

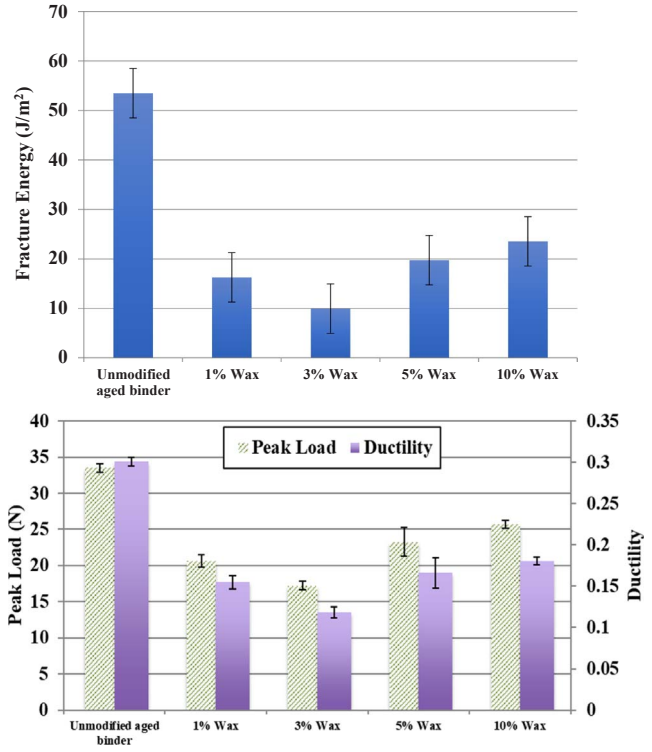

Fig. 4. DTT test results for 0%, 1%, 3%, 5% and 10% wax-modified binder: (a – top) fracture energy, (b – bottom) ductility and peak load.

3.1.5. Size exclusion chromatography (SEC)

Fig. 5 shows the chromatogram of unaged binder, aged binder, and aged binder +10% wax. The figure shows that the peak intensity at early elution time (around 4.91 min) is increasing, and the shoulder around 5.6 min converted to a noticeable peak from unaged to aged binder. But after introducing 10% wax, there is a reduction in the intensity of the areas of both peaks. In size exclusion chromatography, material with a higher molecular weight appears at an earlier elution time. The enhancement in the peak area shows an increase in molecular weight after aging. Table 1 shows the cumulative percentage of area from the start time of elution up to 5.8 min for all three chromatograms. Based on size exclusion analysis, the large molecular size increase after aging, and it was reduced after 10% wax inclusion.

Table 1
Cumulative percentage area of refractive index.

Name of sample	Cumulative % (start of slice to 5.8 min)
Unaged	155.47
Aged	256.66
Aged + 10 wt% Wax	226.02

4. Computational details and analysis

4.1. Molecular dynamics simulation

Molecular dynamics simulation (MDS) was performed on a system at equilibrium state composed of oxidized asphaltene, paraffinic wax, and methanol as a solvent, using Large-scale Atomic and Molecular Massively Parallel (LAMMPS) software in MedeA® environment version 2.2 to investigate the interaction of paraffinic wax molecules as a rejuvenating agent on oxidized asphaltene molecules. The model was built in the MedeA® environment using the molecular builder, which allows an interactive, step-by-step construction of polyaromatic units with attached alkyl chains and thiophenic rings. This study used the PCFF + force field, which is an extension of the PCFF force field. "Force field" refers to the functional form of parameters used to calculate the potential and kinetic energy of the system of atoms and molecules [43]. PCFF+ is an all-atom force field designed to provide excellent accuracy on hydrocarbon and liquid modeling from *ab initio* simulations [48]. It includes a Lenard-Jones 9–6 potential for intermolecular and intramolecular interactions and specific stretching, bending, and torsion terms to involve 1–2, 1–3, and 1–4 interactions.

4.1.1. Methods of analysis

In this study, to study the effect of the presence of wax molecules on the self-association or stacking of oxidized asphaltene molecules, the change in interaction energy and stacking distance of a dimer was measured. The interaction energy of an oxidized asphaltene dimer is a measurement of the thermodynamic stability. The interaction energy (E_{int}) can be calculated by subtraction of the total energy of the complex from the sum of the fragments' energy (Eq. (1)). This method is widely used in other research [23,32,41].

$$E_{int} = E_{complex} - (\sum E_{fragment}) \quad (1)$$

To further investigate the effect of paraffin wax on the self-interaction of oxidized asphaltene molecules, the average aggregation size of

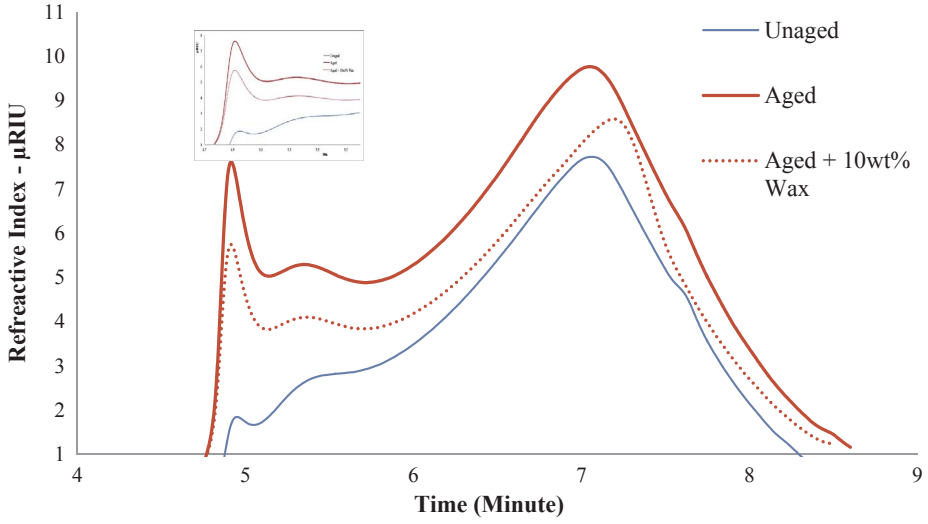

Fig. 5. SEC test results for unaged binder, aged binder, and aged binder +10%wax.

oxidized asphaltene molecules induced with different dosages of wax was calculated. The average aggregation size ($< m >$) was determined according to Eq. (2) [45].

$$< m > = \frac{\sum mN_m}{\sum N_m} \quad (2)$$

where N_m is the number of aggregates containing m oxidized asphaltene molecules

The pairwise radial distribution function or RDF (g(r)) was used in the determination of stacking distance between atoms or molecules. In this study, g(r) was calculated between oxidized asphaltene molecules. The most centered carbon atom on polyaromatic sheet of oxidized asphaltene molecules was used to calculate the RDF.

To examine the mobility of wax molecules in an oxidized asphaltene matrix, first a subset of wax molecules was defined and the mean square displacement (MSD) graph was plotted. Referring to the Einstein relation of Brownian motion and the definition of the diffusion coefficient, the value of the diffusion coefficient was measured according to Eq. (3).

$$D = [Slope\ of\ MSD\ curve\ over\ the\ elapsed\ time\ t]/[2d] \quad (3)$$

where D is the diffusion coefficient, d is dimensionality, and t is the time over which we are calculating the diffusion coefficient. The unit for a diffusion coefficient is $Å^2$/ps (or 10^{-4} cm^2/s).

4.1.2. Structure of oxidized asphaltene, paraffin wax and solvent

The oxidized asphaltene molecule used in this study was proposed by our research group; the molecule's properties and structure were developed recently. It is an oxidized asphaltene-pyrrole including 3 carbonyl groups placed at the most probable locations of the structure [31]. The wax model used in this study as an elementary unit of doped wax is the n-C_{11} paraffin wax that is a polymethylene sequence of –(CH2)- that regularly stacks in layers.

The chain length selected for this research was n-$C_{11}H_{24}$, which has been used before for understanding the interactions between wax and unoxidized asphaltene [32]. The selected wax structure may have a shorter length than the ones actually used for doping asphalt binders, but it helps with regard to the limitations on simulation size and computational cost on simulations that can be conducted. The proposed structures for oxidized asphaltene and n-paraffin wax are shown in Fig. 6.

In this study methanol solvent was used to provide an aggregation effect on oxidized asphaltene molecules. In most asphaltene related researches, n-heptane is the selected solvent but in this study, since the effect of n-C_{11} is of interest, the solvent needed to have a different chemical structure than an aliphatic chain hydrocarbon. Otherwise, the effect of wax molecules will be overlooked.

The geometry of the system of molecules goes through a simple force field minimization and force field dynamics to ensure that none of the atoms are too close to each other.

4.1.3. Simulation method

The interaction energy of a dimer of oxidized asphaltene was studied using a two-stage LAMMPS. The first stage started with an NVT at a high temperature (800 K) for 100 ps and an NPT with a high pressure (200 atm) for 500 ps, both annealed to 298.15 K (25 °C) and 1 atm to shake the system and prevent trapping at local minimum energy states. The second stage of the two-stage LAMMPS was started with an NVT (constant number of atoms, volume, and temperature) ensemble with a temperature of 298.15 K (25 °C) followed by an NPT (constant number of atoms, pressure, and temperature) ensemble with a temperature of 298.15 K (25 °C) and a pressure of 1 atm. The ensemble was composed of two oxidized asphaltene molecules and 600 molecules of methanol as solvent. Methanol was chosen because of its tendency to aggregate oxidized asphaltenes. The NVT duration was 2 ns (ns) to reach an equilibrated state for atomic and molecular configuration, followed by an NPT simulation for 30 ns at 298.15 K (25 °C) and a pressure of 1 atm. To measure the effect of wax on the interaction energy of oxidized molecules, another simulation was performed with the same procedure except for one change: the replacement of 6.5 wt% of methanol solvent with wax molecules. For outcomes, the interaction energy and stacking distance of oxidized asphaltene dimers were measured with and without the presence of wax. An oxidized asphaltene dimer was considered stacked when 50 percent or more of the polyaromatic area was overlapped, which is observable by rotating the configuration around the axis normal to the tangent plane. The stacking distance was measured between the closest points of molecules.

To better understand the effect of wax on the self-association and formation of nano-aggregates of oxidized asphaltene molecules, an ensemble of 17 oxidized asphaltenes, 2000 methanol molecules and a different number of wax molecules equal to 1%, 3%, 5% and 10% by weight fraction of oxidized asphaltene was built. The simulation was performed in two stages with two LAMMPS. The first LAMMPS stage was exactly like the previous method, while the second stage started using an NVT simulation of 2 ns follow up by an NPT simulation of 10 ns, both at 298.15 K (25 °C) and 1 atm. The diffusion analysis was conducted over 1 ns for the wax subset. To have a better understanding of the computational cost, second stage of LAMMPS in simulation was done in 947,481 s (approximately 74 s for each step)

The short-range interactions were calculated directly, and long-

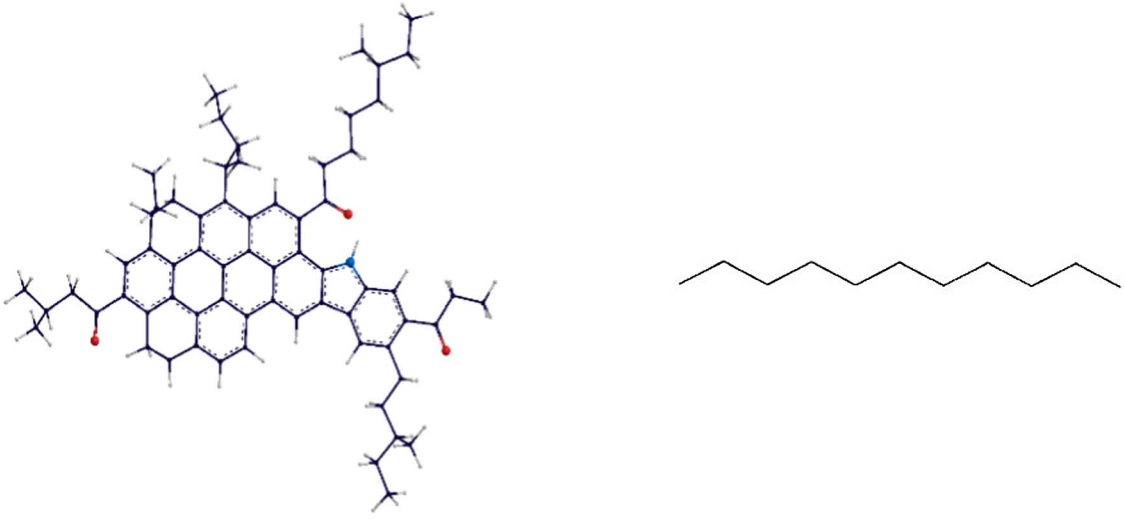

Fig. 6. Oxidized asphaltene (red atoms are oxygens and blue atom is nitrogen) (Left) and wax ($C_{11}H_{24}$) (Right) molecular structures.

range interactions were computed with the particle–particle–particle mesh (PPPM) method. The first-stage molecular calculations were performed initializing with an energy minimization at constant volume using the conjugate gradient method. For the purpose of this study, a Nose-Hoover thermostat and barostat was used to maintain constant temperature and pressure during the simulation. Non-bonded interaction terms were calculated with a simple cutoff of 9.5 Å. The matrix of methanol, oxidized asphaltene, and wax was started with a low average density for both simulation methods to avoid molecular overlaps. In the current study, all the wax molecules were considered as one subset of the whole system, and the mean square displacement was calculated for this subset.

4.2. Molecular dynamics simulation results

4.2.1. Effect of wax on self-association of oxidized asphaltene

The geometric conformation and stability of an oxidized asphaltene dimer in methanol solvent was studied. For comparison purposes, two ensembles were studied: one with methanol only, and one contained wax equal to 6.5 wt% of solvent. The solvent was replaced with wax (instead of just adding wax to the system) to keep the mass ratio equal in both configurations. Fig. 7 illustrates the final configuration of the simulation (solvent molecules are hidden for clarity). The procedure was explained earlier in the methods section. The stacking distance (closest point of polyaromatic sheets) and the interaction energy were calculated and are presented in Table 2. The results for the interaction energy and stacking distance show that the presence of wax molecules (or n-alkanes in general) promotes dimerization of oxidized asphaltene molecules. The interaction energy of an oxidized asphaltene dimer is showing that the dimer that is formed in the presence of wax molecules is more stable than the one formed in undoped solvent. The stacking distance also shows the same trend; its value is lower when wax molecules are around asphaltene molecules. These results show that wax by itself doesn't have a peptizing effect on oxidized asphaltene molecules, because wax brings an oxidized asphaltene dimer to a lower energy state and stabilizes it.

To evaluate the effect of n-paraffin wax on the formation of nanoaggregates of oxidized asphaltene, a system of oxidized asphaltene molecules, wax molecules, and methanol as solvent was studied. Each ensemble was composed of 2000 molecules of methanol, 17 molecules of oxidized asphaltene, and 1 to 10 molecules of paraffin wax as a weight fraction of the oxidized asphaltene molecules (1%, 3%, 5%, and 10% of oxidized asphaltene molecules weight fractions). The simulation procedure was elaborated in the simulation methods section. The

Table 2
Interaction energy for oxidized asphaltene dimer and stacking distance without and with the presence of wax.

Measurement	Oxidized asphaltene dimer without wax in solvent	Oxidized asphaltene dimer with 6.5 wt% of solvent replaced with wax
Interaction energy (kJ/mol)	−15	−58
Stacking distance (Å)	3.267	3.166

results of the number of formed nanoaggregate and the average aggregation size are shown in Fig. 8. The results show a reduced size of aggregation (number of molecules forming a nanoaggregate) after adding wax to the system of oxidized asphaltene in solvent. Although the results show a general reduction in size, a specific trend was not observed. The results also show that by adding wax to the system, oxidized asphaltene molecules pack in a smaller size of nanoaggregates but nanoaggregates become more frequent.

4.2.2. Radial distribution function (pair correlation function)

To obtain better insight into the aggregation of oxidized asphaltene molecules with and without presence of wax molecules, the radial distribution function (RDF), g(r), was calculated for the system with just oxidized asphaltene and another with 10 wt% wax relative to asphaltene portion. Fig. 9 illustrates the results of the RDF analysis. The most centered carbon atom of polyaromatic sheet of oxidized asphaltene molecules was selected as a subset to calculate RDF. The results show that addition of wax content results in higher probability of stacking of oxidizied asphaltene molecules at lower distance. The intensity of occurrence of π-π stack of oxidized asphaltene molecules (first peak) at distance of 4.6 Å is higher in presence of wax molecules compared to the ensemble without wax which is aligned with results of interaction energy. The second peak may represent the T-shaped stacking of asphaltene molecules which occurs at 7.3 Å.

4.2.3. Diffusion analysis

Using Eq. (3), the mean squared displacement (MSD) of the wax subset was calculated for 1 ns to evaluate the diffusion coefficient of the wax molecules in an ensemble of oxidized asphaltene and solvent. The purpose of this analysis was to study the effect of an increase of wax concentration on the diffusion of wax molecules into the oxidized asphaltene matrix in solvent. The results of the diffusion coefficient are shown in Table 3. The results indicate that the diffusion of wax

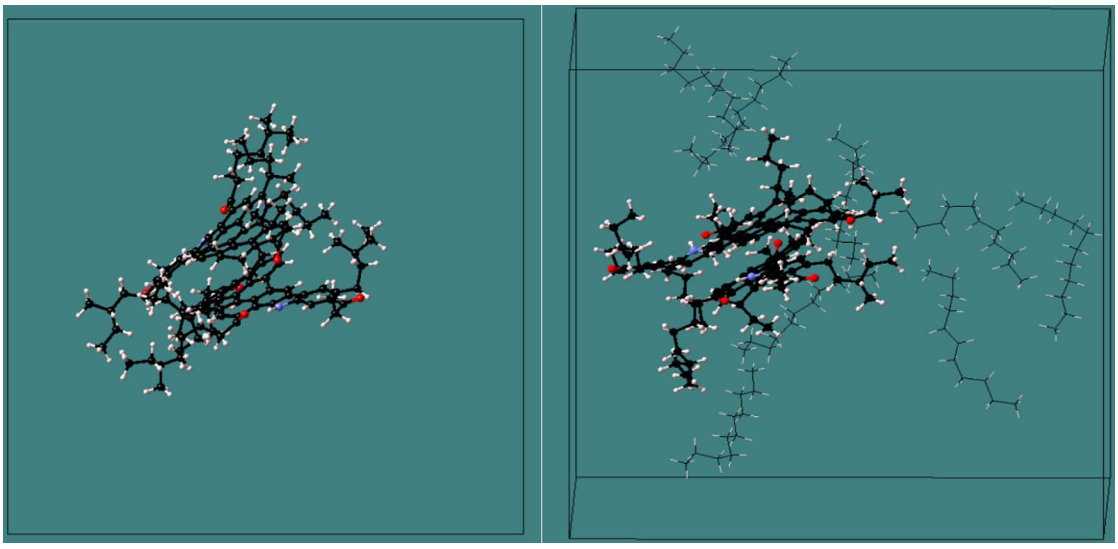

Fig. 7. The final configuration of a dimer of oxidized asphaltene in methanol solvent: (a – left) without wax, (b – right) with the presence of wax.

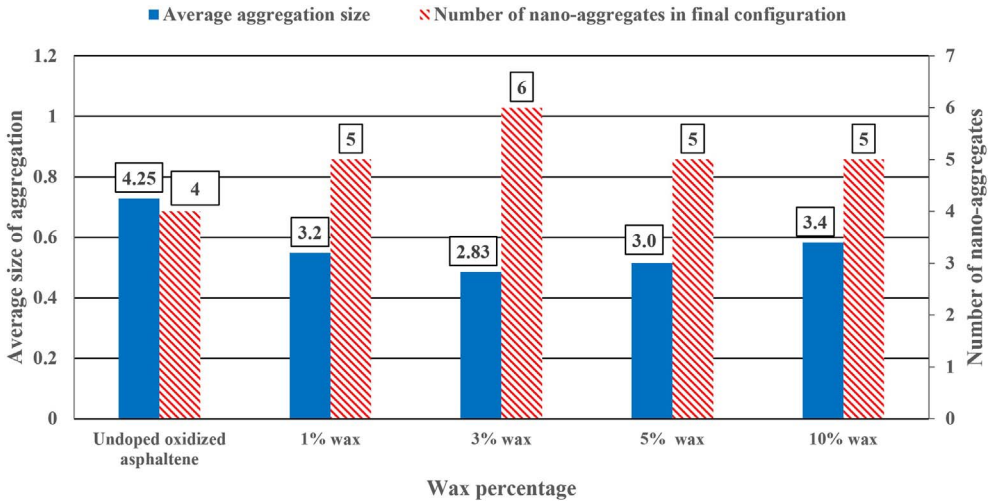

Fig. 8. Average aggregation size (number of molecules forming a nano-aggregate) and number of nano-aggregates in final configuration versus wax weight fraction of oxidized asphaltene in methanol solvent at 298.15 K (25 °C).

molecules increases as the wax concentration increases. This can be attributed to the alteration of aggregates size due to presence of wax. Accordingly, the diffusion coefficient results are in-line with the trend observed for the change of nanoaggregate size as the wax content increases. It was shown that nanoaggregates size decreases 20% when wax content increases from 0% to 10%. In the same token, it was observed that by increasing the wax concentration from 1% to 10%, the diffusion of wax increases by over 100%.

Table 3
Diffusion Coefficient and Calculated Uncertainty of Wax Molecules Within the Wax and Oxidized Asphaltene Matrix in Solvent at 298.15 K (25 °C) (10^{-5} cm^2/s).

Wax concentration	1%	3%	5%	10%
Diffusion coefficient	0.632	0.640	1.115	1.473
Uncertainty	0.022	0.0078	0.0051	0.0078

5. Summary and conclusions

In this paper effects of paraffin wax on molecular conformation and thermo-mechanical properties of oxidized asphalt was examined via computational and laboratory experiments. It has been documented that introduction of paraffin wax can improve the workability of the asphalt mixture allowing for lowering the mixing and compaction temperatures in high RAP mixtures. Accordingly, this paper provides an in-depth examination of the interaction mechanisms between n-paraffin wax and oxidized asphaltene molecules to explain how wax molecules alter thermo-mechanical properties of asphalt binder. Following conclusion were drawn based on computational and laboratory experiments:

- Viscosity results from the RV test show that at high temperature, the viscosity decreases as more wax is added to the aged asphalt binder.
- The complex modulus decreased as the wax concentration increased. This increase is more noticeable at wax content above 3%. The complex modulus results show an overall softening effect (at temperature ranges of 10–76 °C) as wax content increased. Observed softening effect at high and intermediate temperature may be attributed to enhanced dimerization of asphaltene while suppressing formation of asphaltene nano-aggregates.
- Based on molecular dynamics simulation results, the interaction energy of the oxidized asphaltene dimer reached a lower state and their π-π stacking distance decreased from 3.267 Å to 3.166 Å in presence of wax molecules. This can be attributed to the role of paraffinic wax molecules to promote dimerization of oxidized asphaltene molecules.
- The average aggregation size of oxidized asphaltene molecules

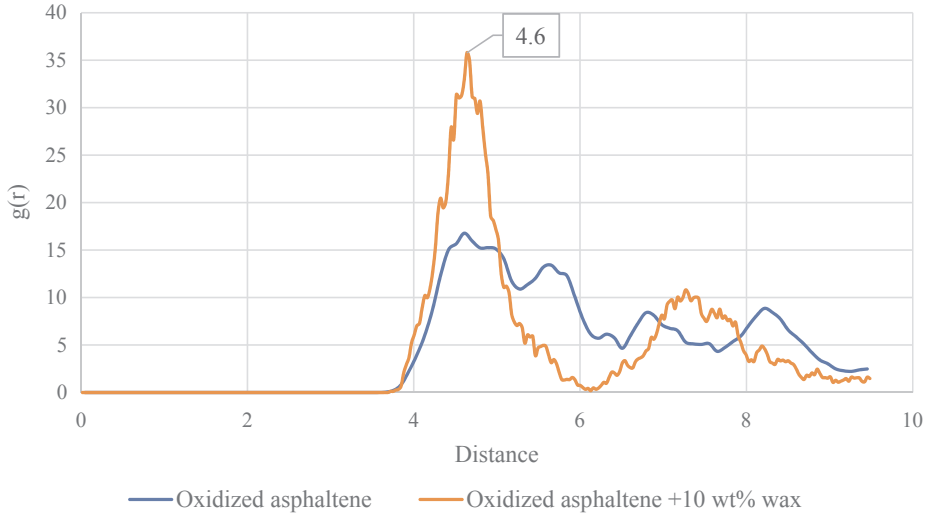

Fig. 9. Oxidized asphaltene molecules g(r) after 10 ns simulation time in methanol solvent at 298.15 K (25 °C).

decreased nearly 20% when wax concentration increased from 0% to 10%. This shows the ability of wax molecules to prevent the formation of nanoaggregates of oxidized asphaltene when they have enough mobility. This phenomenon was observed in size exclusion chromatography showing that introduction of wax reduced large molecule size (LMS) in oxidized binder.

- Moreover, the diffusion coefficient of the paraffin wax molecules increased with increasing wax concentration. The results show an increase of over 100% when the wax content increases from 1% to 10%. This can be attributed to molecular conformation and relative change of nano-aggregate size in presence of wax.
- The radial distribution function of oxidized asphaltene molecules showed the first peak appeared at 4.6 Å corresponding to stacking distance of asphaltene molecules. It was further observed that when wax was introduced to the system, (at 10 wt% dosage), the intensity of the aforementioned peak increased suggesting that addition of wax promotes dimerization by increasing interactions between oxidized asphaltene molecules. The latter observation combined with reduced average nano-aggregates size is reflected in observed rheological changes including overall reduction in complex modulus as well as improved workability of oxidized asphalt binder doped with wax at high and intermediate temperature; aforementioned molecular level interaction mechanism was further verified by size exclusion chromatography.

Following conclusion were derived from laboratory experiments at temperature ranges for which simulations could not be performed due to extensive computational time requirement:

- The stiffness results of the aged binder measured using a bending beam rheometer (at temperature of −12 °C) show a consistent increase by increasing the wax content. The ability to relax stress (known as the m-value) decreased with an increase of wax content in aged binder.
- The fracture energy of the aged binder, measured with a direct tension test (at temperature of −12 °C), decreased after adding paraffin wax. This can be further attributed to a change in fracture mechanism from asphalt-dominant fracture to wax-dominant fracture mechanism. Weak secondary bonds between wax and asphaltene molecules may play as stress localization points giving rise to crack nucleation at wax-asphalt interface leading to low fracture energy. Introduction of wax also resulted in lower ductility in aged asphalt, which continued to decrease with increasing wax percentage.
- The crossover temperature of aged binder show a decreasing trend with introduction of 1% and 3% wax; however, this trend follows with a sudden increase to a temperature even higher than that of the control specimen (aged asphalt with no wax added)) for 5% and 10% wax-doped asphalt samples. The latter change may indicate at certain wax dosage above 3%, thermo-mechanical properties of specimen is controlled by structuring of wax molecules which is also evidenced by fracture properties showing a tipping point at specific wax dosage. The result of study can provide insights on importance of defining critical wax dosage to optimize efficacy of wax-based additives.

Acknowledgements

This research is sponsored by the National Science Foundation – United States (Awards No: 1150695 & 1546921). The authors are grateful for valuable assistance of Shahrzad Hosseinnezhad of North Carolina A&T state university for performing size exclusion chromatography. in addition, the assisatance of Ray Shan with Material Design is highly appreciated..

References

[1] Allen RG, Little DN, Bhasin A, Glover CJ. The effects of chemical composition on asphalt microstructure and their association to pavement performance. Int J Pavement Eng 2014;15(1):9–22.
[2] ASTM D2872–12e1, Standard Test Method for Effect of Heat and Air on a Moving Film of Asphalt (Rolling Thin-Film Oven Test). ASTM International; 2013.
[3] ASTM D4402, Standard Test Method for Viscosity Determination of Asphalt at Elevated Temperatures Using a Rotational Viscometer. ASTM International; 2015.
[4] ASTM D6723–12, Standard Test Method for determining the fracture properties of asphalt binder in direct tension. ASTM International; 2012.
[5] ASTM D6521–13 Standard Practice for Accelerated Aging of Asphalt Binder Using a Pressurized Aging Vessel (PAV). ASTM International; 2016.
[6] ASTM D6648, Standard Test Method for Determining the Flexural Creep Stiffness of Asphalt Binder Using the Bending Beam Rheometer (BBR). ASTM International; 2016.
[7] ASTM D7552–09, Standard Test Method for Determining the Complex Shear Modulus (G∗); Of Bituminous Mixtures Using Dynamic Shear Rheometer. ASTM International; 2014.
[8] Bowers BF, Huang B, Shu X. Refining laboratory procedure for artificial RAP: a comparative study. Constr Build Mater 2014;52:385–90.
[9] Chen M, Xiao F, Putman B, Leng B, Wu S. High temperature properties of rejuvenating recovered binder with rejuvenator, waste cooking and cotton seed oils. Constr Build Mater 2014;59:10–6.
[11] De Filippis P, Giavarini C, Scarsella M. Improving the ageing resistance of straight-run bitumens by addition of phosphorus compounds. Fuel 1995;74(6):836–41.
[12] De Moraes M, Pereira R, Simão R, Leite L. High temperature AFM study of CAP 30/45 pen grade bitumen. J Microsc 2010;239(1):46–53.
[13] Durrieu F, Farcas F, Mouillet V. The influence of UV aging of a styrene/butadiene/styrene modified bitumen: comparison between laboratory and on site aging. Fuel 2007;86(10):1446–51.
[14] Eberhardsteiner L, Füssl J, Hofko B, Handle F, Hospodka M, Blab R, et al. Influence of asphaltene content on mechanical bitumen behavior: experimental investigation and micromechanical modeling. Mater Struct 2015;48(10):3099–112.
[15] Fischer HR, Dillingh E, Hermse C. On the microstructure of bituminous binders. Road Mater Pavement Des 2014;15(1):1–15.
[16] Gawel I, Czechowski F. Wax content of bitumens and its composition. Erdoel Erdgas Kohle 1998;114(10):507–9.
[17] Huang SC, Qin Q, Grimes WR, Pauli AT, Glaser R. Influence of rejuvenators on the physical properties of RAP binders. J Test Eval 2014;43(3):594–603.
[18] Hofko B, Eberhardsteiner L, Füssl J, Grothe H, Handle F, Hospodka M, et al. Impact of maltene and asphaltene fraction on mechanical behavior and microstructure of bitumen. Mater Struct 2016;49(3):829–41.
[19] Houston W, Mirza M, Zapata C, Raghavendra S. Simulating the effects of hot mix asphalt aging for performance testing and pavement structural design. NCHR Research Results Digest, 324; 2007.
[20] Laukkanen OV. Small-diameter parallel plate rheometry: a simple technique for measuring rheological properties of glass-forming liquids in shear. Rheol Acta 2017;56(7–8):661–71.
[22] Li DD, Greenfield ML. Chemical compositions of improved model asphalt systems for molecular simulations. Fuel 2014;115:347–56.
[23] Liu J, Zhao Y, Ren S. Molecular dynamics simulation of self-aggregation of asphaltenes at an oil/water interface: formation and destruction of the asphaltene protective film. Energy Fuels 2015;29(2):1233–42.
[25] Mogawer WS, Austerman A, Roque R, Underwood S, Mohammad L, Zou J. Ageing and rejuvenators: evaluating their impact on high RAP mixtures fatigue cracking characteristics using advanced mechanistic models and testing methods. Road Mater Pavement Des 2015;16(sup2):1–28.
[26] Mullins OC. The modified Yen model. Energy Fuels 2010;24(4):2179–207.
[27] National Asphalt Pavement Association. Sustainability Report: Black and Green: Sustainable Asphalt, Now and tomorrow. http://www.asphaltpavement.org/index.php?option=com_content&view=article&id=493&Itemid=100305 (Accessed January 2, 2018).
[28] Oklahoma department of transportation. Monthly asphalt binder price index. http://www.okladot.state.ok.us/contractadmin/pdfs/binder-index.pdf (Accessed January 2, 2018).
[29] Oldham D, Fini EH, Abu-Lebdeh T. Investigating the rejuvenating effect of bio-binder on recycled asphalt shingles (No. 14–3775); 2014.
[30] Oldham DJ. The Feasibility of Rejuvenating Aged Asphalt with Bio-Oil from Swine Manure (Doctoral dissertation, North Carolina Agricultural and Technical State University); 2015.
[31] Pahlavan F, Mousavi M, Hung A, Fini E. Characterization of oxidized asphaltenes and the restorative effect of a bio-modifier. RSC Adv 2017. (Accepted with revision).
[32] Pahlavan F, Mousavi M, Hung A, Fini EH. Investigating molecular interactions and surface morphology of wax-doped asphaltenes. PCCP 2016;18(13):8840–54.
[33] Pauli A, Grimes R, Beemer A, Turner T, Branthaver J. Morphology of asphalts, asphalt fractions and model wax-doped asphalts studied by atomic force microscopy. Int J Pavement Eng 2011;12(4):291–309.
[34] Petersen JC. A review of the fundamentals of asphalt oxidation: chemical, physicochemical, physical property, and durability relationships. Transp Res. E (E-C140); 2009.
[35] Qin Q, Schabron JF, Boysen RB, Farrar MJ. Field aging effect on chemistry and rheology of asphalt binders and rheological predictions for field aging. Fuel 2014;121:86–94.

[36] Ruan Y, Davison RR, Glover CJ. The effect of long-term oxidation on the rheological properties of polymer modified asphalts☆. Fuel 2003;82(14):1763–73.
[37] Samieadel A, Oldham D, Fini EH. Multi-scale characterization of the effect of wax on intermolecular interactions in asphalt binder. Constr Build Mater 2017;157:1163–72.
[38] Schmets A, Kringos N, Pauli T, Redelius P, Scarpas T. On the existence of wax-induced phase separation in bitumen. Int J Pavement Eng 2010;11(6):555–63.
[39] Sharma BK, Ma J, Kunwar B, Singhvi P, Ozer H, Rajagopalan N. Modeling the Performance Properties of RAS and RAP Blended Asphalt Mixes Using Chemical Compositional Information (0197–9191); 2017. Retrieved from.
[40] Siddiqui MN, Ali MF. Studies on the aging behavior of the Arabian asphalts. Fuel 1999;78(9):1005–15.
[41] Silva HS, Sodero AC, Bouyssiere B, Carrier H, Korb J-P, Alfarra A, et al. Molecular dynamics study of nanoaggregation in asphaltene mixtures: effects of the N, O, and S Heteroatoms. Energy Fuels 2016;30(7):5656–64.
[42] Speight JG. The chemical and physical structure of petroleum: effects on recovery operations. J Petrol Sci Eng 1999;22(1):3–15.
[43] Sun H, Mumby SJ, Maple JR, Hagler AT. An ab initio CFF93 all-atom force field for polycarbonates. J Am Chem Soc 1994;116(7):2978–87.
[44] Traxler R. Relation between asphalt composition and hardening by volatilization and oxidation. In: Paper presented at the Assoc Asphalt Paving Technol Proc; 1961.
[45] Ungerer P, Rigby D, Leblanc B, Yiannourakou M. Sensitivity of the aggregation behaviour of asphaltenes to molecular weight and structure using molecular dynamics. Mol Simul 2014;40(1–3):115–22.
[46] Vaitkus A, Cygas D, Laurinavicius A, Perveneckas Z. Analysis and evaluation of possibilities for the use of warm mix asphalt in Lithuania. Baltic J Road Bridge Eng 2009;4(2):80–6.
[47] Vargas X, Afanasjeva N, Álvarez M, Marchal P, Choplin L. Asphalt rheology evolution through thermo-oxidation (aging) in a rheo-reactor. Fuel 2008;87(13):3018–23.
[48] Waldman M, Hagler AT. New combining rules for rare gas van der Waals parameters. J Comput Chem 1993;14(9):1077–84.
[49] Wang PY, Zhao K, Glover C, Chen L, Wen Y, Chong D, et al. Effects of aging on the properties of asphalt at the nanoscale. Constr Build Mater 2015;80:244–54.
[50] Wang W, Chen J, Sun Y, Xu B, Li J, Liu J. Laboratory performance analysis of high percentage artificial RAP binder with WMA additives. Constr Build Mater 2017;147:58–65.
[51] Williams ML, Landel RF, Ferry JD. The temperature dependence of relaxation mechanisms in amorphous polymers and other glass-forming liquids. J Am Chem Soc 1955;77(14):3701–7.
[52] Xu G, Wang H. Molecular dynamics study of oxidative aging effect on asphalt binder properties. Fuel 2017;188:1–10.
[53] Zaumanis M, Mallick R, Frank R. Evaluation of rejuvenator's effectiveness with conventional mix testing for 100% reclaimed asphalt pavement mixtures. Transp Res Record 2013;2370:17–25.